

Electronic Supplementary Information

Solution Properties of Imidazolium-Based Amphiphilic Polyelectrolyte in Pure- and Mixed-Solvent Media

Chien-You Su,^a Han-Liou Yi,^a Li-Duan Tsai,^b Ming-Chou Chen*^c and Chi-Chung Hua*^a

^aDepartment of Chemical Engineering, National Chung Cheng University, Chia-Yi 62102, Taiwan,
ROC.

^bMaterial and Chemical Research Laboratories, Industrial Technology Research Institute, Hsinchu
31040, Taiwan, ROC.

^cDepartment of Chemistry, National Central University, Jhong-Li 32001, Taiwan, ROC.

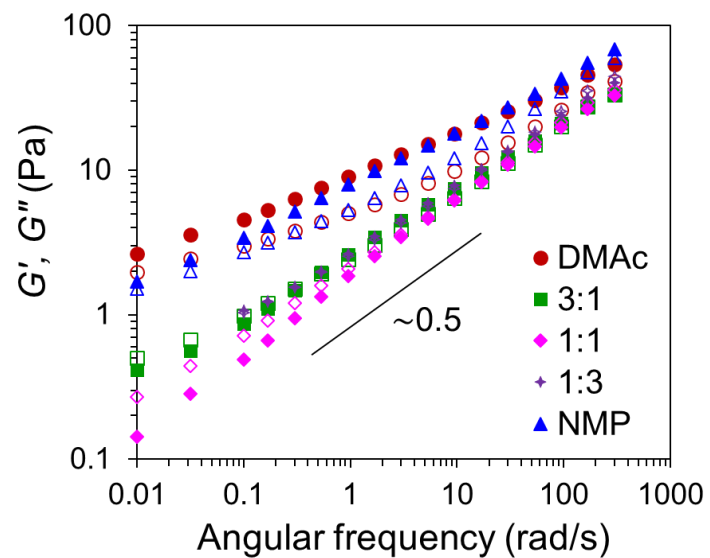


Fig. S1 Dynamic modulus responses, G' (solid symbols) and G'' (open symbols), as functions of the angular frequency for the 4 wt% polyelectrolyte solutions with various blending (volume) ratios of DMAC and NMP.

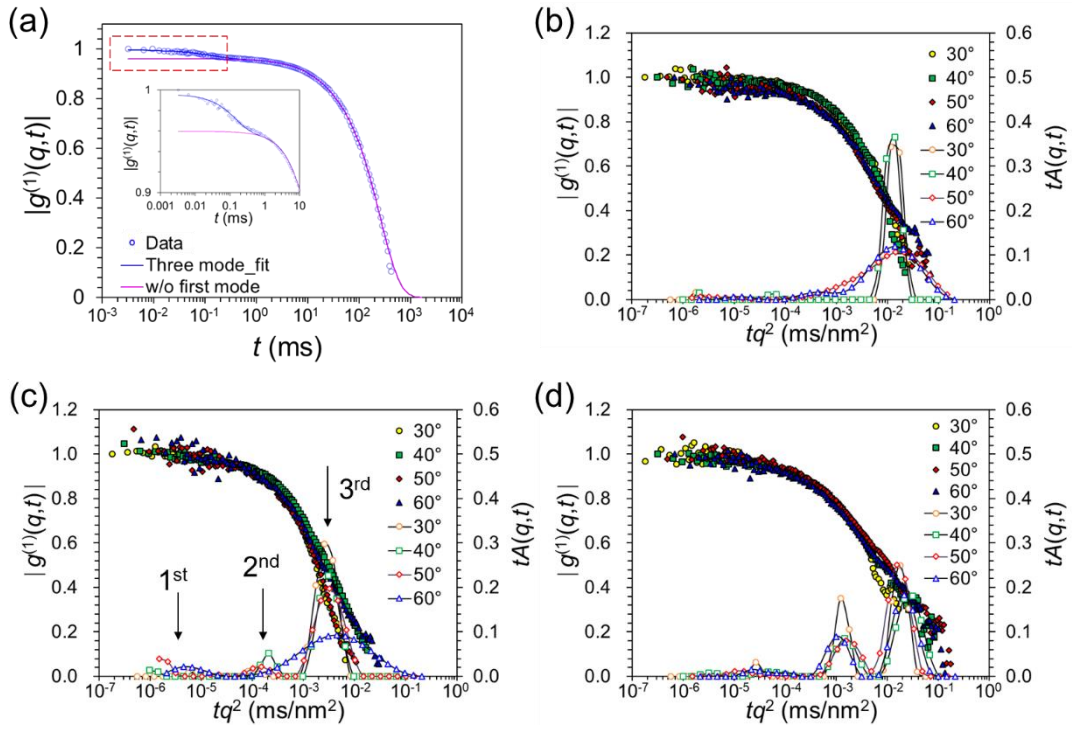


Fig. S2 (a) Field autocorrelation function at a small scattering angle of $\theta = 30^\circ$ for the 1 wt% polyelectrolyte solution prepared with the 1:1 DMAc/NMP medium. The fitted curves, with or without including the first-mode contribution, using the Kohlrausch-Williams-Watts (KWW) function demonstrate the necessity of including all three relaxation modes. The inset shows the zoomed-in plot of the marked area in the main plot, indicating a drastic difference between the two fitted curves. (b-d) Angular dependences of the field autocorrelation function and the associated decay time distribution extracted from CONTIN for the 0.1 wt% polyelectrolyte solutions prepared with (b) DMAc, (c) 1:1 DMAc/NMP, and (d) NMP, where the decay time t has been rescaled with q^2 . The arrows in (c) designate three relaxation modes representing polyion, aggregate, and cluster, respectively. Material properties extracted for these (dilute) solutions are gathered in the table below.

Solvent	$R_{H, \text{ion}}$ (nm)	$R_{H, \text{agg}}$ (nm)	$R_{H, \text{cluster}}$ (nm)	W_{ion}	W_{agg}	W_{cluster}	ion-to-cluster ratio
DMAc	1.0±0.1	n/a	3600±200	67%	0%	33%	2.05
1:1	1.0±0.1	62±8	1500±100	85%	10%	5%	17.06
NMP	2.4±0.2	115±8	2300±200	77%	18%	5%	15.40

UV-vis absorption spectra for the polyelectrolyte solutions: Fig. S3 shows the UV-vis absorption spectra for the 0.1 and 1 wt% polyelectrolyte solutions prepared with DMAc, 1:1 DMAc/NMP, and NMP, respectively. For imidazolium-based polyelectrolytes, the absorption spectra were previously reported to be especially sensitive to the electronic transitions arising from the imidazolium-ring association.^{1,2} Accordingly, the primary absorption peak at ~240 nm for the present polyelectrolyte solutions may be attributed to the aggregates consisting of imidazolium ions,^{1,2} as it becomes more pronounced with increased polyelectrolyte concentration. It can also be seen that only the solutions prepared with the 1:1 DMAc/NMP and NMP media exhibit a second peak at ~290 nm, indicating a better solvation of the imidazolium group in these two media than in DMAc.¹ With increased polyelectrolyte concentration, this peak becomes more pronounced and the peak height is greater in NMP than in 1:1 DMAc/NMP. These observations are in accord with the solvent quality inferable from the polyelectrolyte conformation resolved in the structural (SAXS) analysis discussed in the main text, namely, the solvent quality for 1:1 DMAc/NMP falls somewhere in between those of DMAc and NMP.

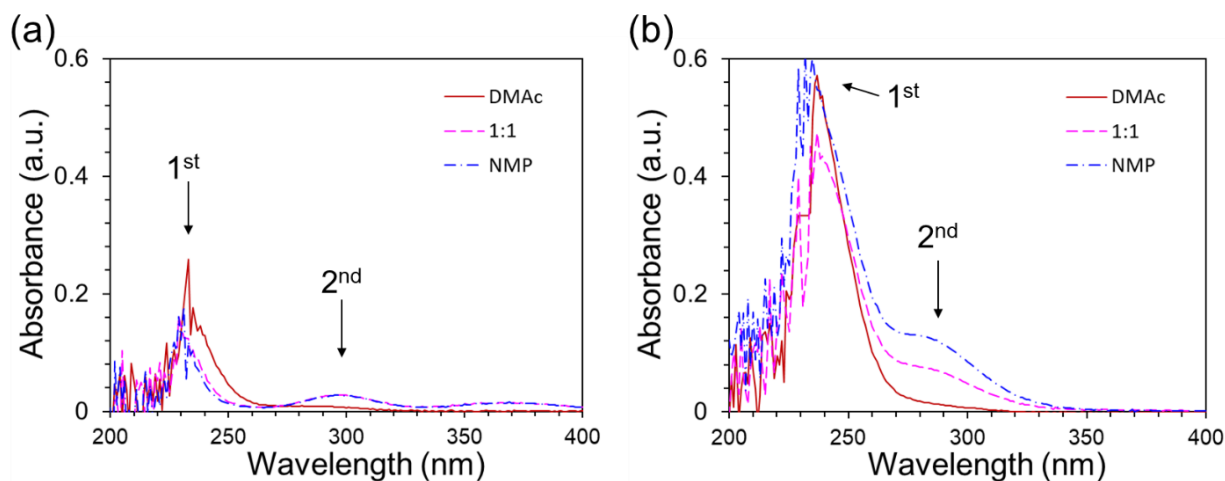


Fig. S3 UV-vis absorption spectra of the (a) 0.1 wt% and (b) 1 wt% polyelectrolyte solutions prepared with DMAc, 1:1 DMAc/NMP, and NMP, respectively. The absorption peaks at ~ 240 nm and ~ 290 nm as indicated by the arrows may be attributed to the aggregates of cationic imidazolium group and the solvation of this group, respectively.

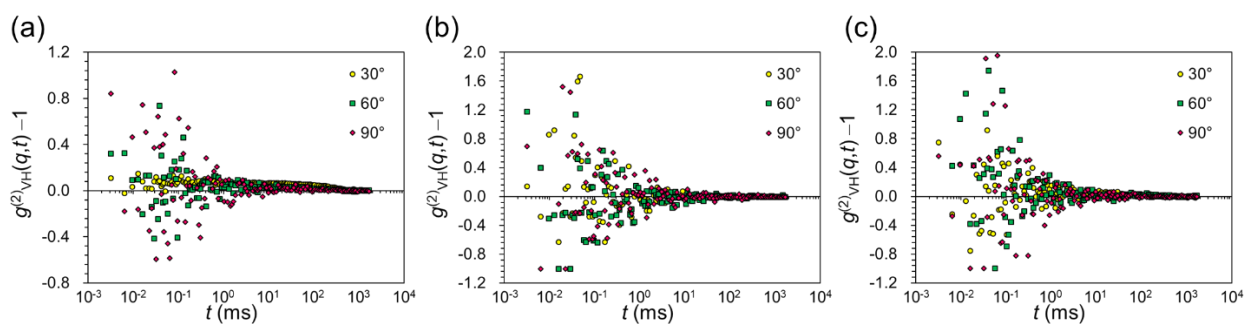


Fig. S4 Depolarized intensity correlation functions, $g_{VH}^{(2)}(q,t) - 1$, for the 1 wt% polyelectrolyte solutions prepared with (a) DMAc, (b) 1:1 DMAc/NMP, and (c) NMP at the scattering angles of $\theta = 30^\circ$, 60° , and 90° . No discernible relaxation patterns are found in all three cases.

Model fits of SALS/SLS/SAXS data: In eqn (1) of the main text, $I_{\text{chain}}(q)$ reflects the internal structure of polyelectrolyte chains and can be described by the combination of the form factor for wormlike chains and a structure factor accounting for the effect of segmental correlations (which produce the peak in SAXS profiles), with a constant factor k_i :

$$I_{\text{chain}}(q) = k_1 S_{\text{electrostatic}}(q) P_{\text{wormlikechain}}(q) \quad (\text{S1})$$

As reported previously,³⁻⁵ the transition from (local) rigid-rod to (global) Gaussian conformation of a wormlike chain may be captured by using the Sharp and Bloomfield function:⁶

$$P_{\text{SB}}(q) = 2 \frac{e^{-x} + x - 1}{x^2} + \frac{2l_p}{15l_c} \left[4 + \frac{7}{x} - \left(11 + \frac{7}{x} \right) e^{-x} \right], \text{ for } ql_c < 2 \quad (\text{S2})$$

and the asymptotic (high- q) region is described by the des Cloizeaux expression:⁷

$$P_{\text{Cloizeaux}}(q) = \frac{\pi}{ql_p} + \frac{2}{3q^2 l_p l_c}, \text{ for } ql_c > 2 \quad (\text{S3})$$

where l_p is the persistence length, l_c is the contour length, and $x = l_c l_p q^2 / 3$ with $l_c > 10 l_p$. The simplest electrostatic structure factor that accounts for the segmental correlations manifested by the SAXS peak is given by^{8,9}

$$S(q) = \frac{1}{1 + C \cdot \exp[-(q\xi)^2]} \quad (\text{S4})$$

where C is a constant, and ξ represents the electrostatic correlation length. The combination of eqn (S1)-(S4) has been applied successfully to describing the chain conformation of a natural polyelectrolyte system.³

The $I_{\text{agg}}(q)$ in eqn (1) accounts for the mass-fractal structure of an aggregate species and may be described by the product of a form factor and structure factor ($S_{\text{fractal}}(q)P_{\text{packing}}(q)$):

$$I_{\text{agg}}(q) = k_2[S_{\text{fractal}}(q)P_{\text{packing}}(q)] \quad (\text{S5})$$

In eqn (S5), a rather general structure factor describing mass-fractal structures is employed:¹⁰

$$S(q) = 1 + \frac{D_{\text{m,agg}}\Gamma(D_{\text{m,agg}} - 1) \sin[(D_{\text{m,agg}} - 1) \tan^{-1}(q\zeta)]}{(qr_0)^{D_{\text{m,agg}}} (1 + 1/(q\zeta)^2)^{(D_{\text{m,agg}}-1)/2}} \quad (\text{S6})$$

where $D_{\text{m,agg}}$ denotes the mass-fractal dimension of an average aggregate, ζ represents the cut-off distance beyond which the mass-fractal structure ceases to apply, and r_0 reflects the dimension of the constituting polyelectrolyte chains. For simplicity, the form factor $P_{\text{packing}}(q)$ in eqn (S5), which describes the conformation of the constituting chains, utilizes the Debye function for a Gaussian chain:

$$P_{\text{packing}}(q) = \frac{2}{(qR_{\text{g,packing}})^4} [\exp(-q^2R_{\text{g,packing}}^2) - 1 + q^2R_{\text{g,packing}}^2] \quad (\text{S7})$$

The resulting chain dimension ($R_{\text{g,packing}} \sim 12$ nm) agrees reasonably with that estimated from the wormlike chain model ($R_{\text{g,chain}} \sim 15$ nm); see **Table 2** in the main text.

For the contribution of cluster species, $I_{\text{cluster}}(q)$ is described by the Guinier-Porod model for three-dimensional objects:¹¹

$$I(q) = G \exp\left(\frac{-q^2R_{\text{g,cluster}}^2}{3}\right), \text{ for } q \leq q_1 \quad (\text{S8})$$

$$I(q) = \frac{B}{q^{D_{\text{m,cluster}}}}, \text{ for } q \geq q_1$$

$$q_1 = \frac{1}{R_{\text{g,cluster}}} \left(\frac{3D_{\text{m,cluster}}}{2}\right)^{1/2}$$

where G and B denote the Guinier and Porod scale factors, respectively, and $D_{\text{m,cluster}}$ represents the mass-fractal exponent for the cluster interior. The model fits that show the contribution of the individual species are shown in **Fig. S5**, with the full set of fitted parameters given in **Table S1**.

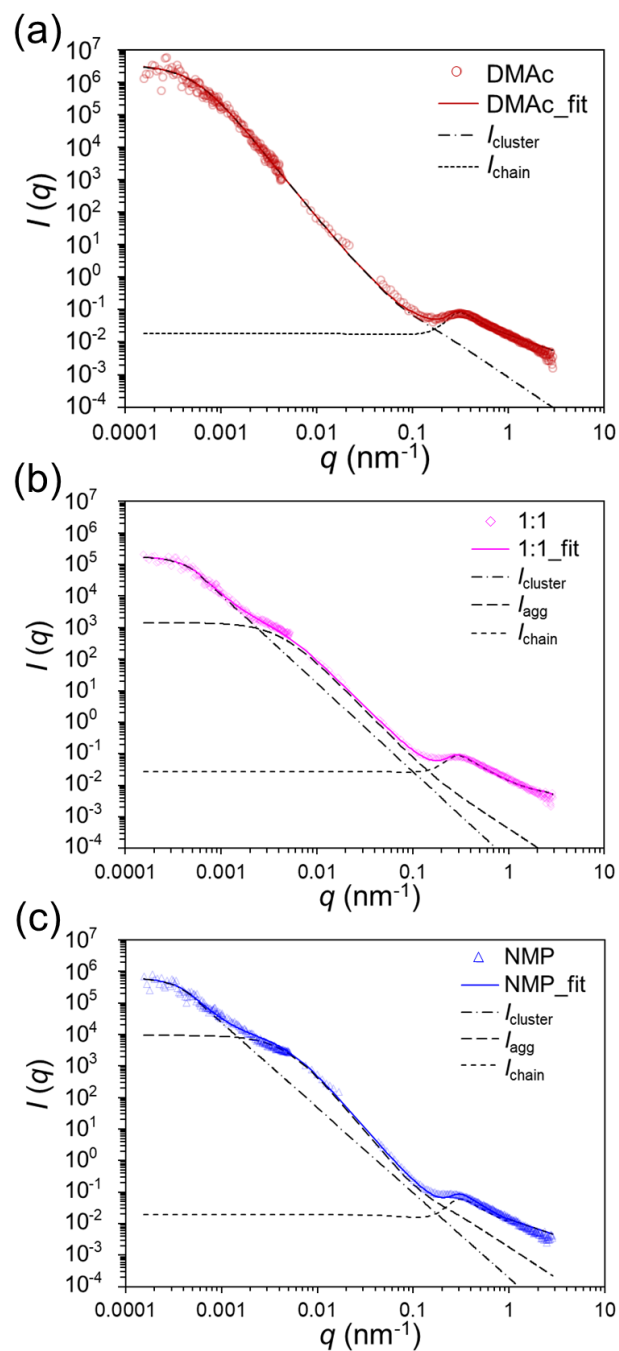


Fig. S5 Combined SALS/SLS/SAXS intensity profiles for the 1 wt% polyelectrolyte solutions prepared with (a) DMAC, (b) 1:1 DMAC/NMP, and (c) NMP, where the dash-dotted, long-dashed, and dashed lines indicate the model fits for the individual contribution from cluster, aggregate, and polyion species, respectively. Note that for the DMAC medium there is no contribution from the intermediate aggregate species, as suggested by the DLS analysis.

Table S1 Full set of fitted parameters determined from the model fits shown in **Fig. 4** of the main text

using eqn(1)

	Parameters	DMAc	1:1	NMP
I_{chain}	k_1	0.962±0.085	0.940±0.037	0.956±0.045
	$R_{\text{g,chain}}$ (nm)	15.1	14.7	15.3
	l_c (nm)	245.0±21.6	273.6±10.8	319.0±14.9
	l_p (nm)	2.8±0.2	2.4±0.1	2.2±0.1
	ξ (nm)	7.8±0.7	7.2±0.3	7.6±0.4
	C	60.9±5.4	28.1±1.1	32.8±2.3
I_{agg}	k_2	0.067±0.006 ^a	0.027±0.001	0.065±0.003
	$R_{\text{g,agg}}$ (nm)	n/a	521	447
	ζ (nm)	1793±158 ^a	226±9	200±9
	$D_{\text{m,agg}}$	n/a	2.6±0.1	2.9±0.1
	$R_{\text{g,packing}}$ (nm)	12.8±1.1 ^a	11.1±0.4	13.4±0.6
	ρ_{agg}	n/a	2.58 ^b	6.77 ^b
I_{cluster}	G ($\times 10^5$)	34.41±3.04 ^c	1.87±0.07	6.54±0.31
	B ($\times 10^{-5}$)	18.73±1.65 ^c	3.52±0.14	18.97±0.89
	q_1 (nm ⁻¹)	0.00054 ^c	0.00060	0.00048
	$R_{\text{g,cluster}}$ (nm)	3910±345 ^c	3430±135	4160±190
	$D_{\text{m,cluster}}$	2.9±0.3	2.8±0.1	2.7±0.1
	ρ_{cluster}	0.48	1.32	1.04

^aThese results for DMAc actually represent the properties of the cluster species; see notes in the main text.^bThis ratio for the aggregate species could be subjected to large uncertainties because of its trace amount in the DLS analysis.^cThese results for DMAc are re-fitted using the Guinier-Porod model in order to facilitate a direct comparison with those for the 1:1 DMAc and NMP media.

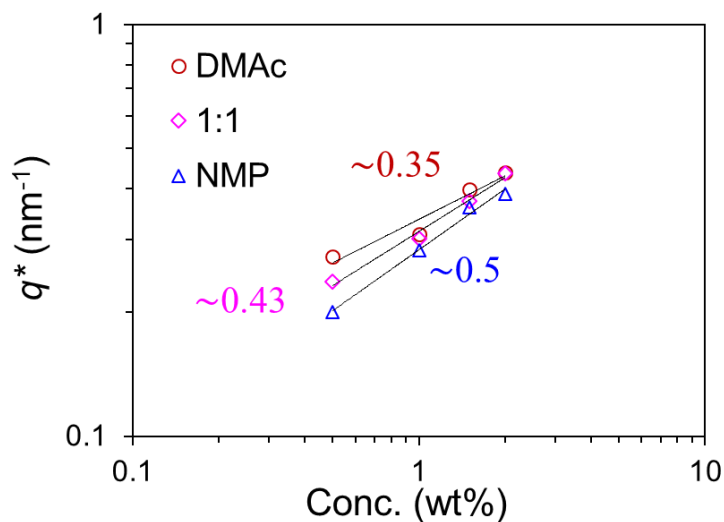


Fig. S6 Scaling relationships between q^* and the polyelectrolyte concentration for polyelectrolyte solutions prepared with DMAc, 1:1 DMAc/NMP, and NMP, where the solid lines denote the results of a power-law fit.

References

- 1 H. Zhang, H. Liang, J. Wang and K. Li, in *Zeitschrift für Physikalische Chemie*, 2007, vol. 221, p. 1061.
- 2 M. A. Rather, G. M. Rather, S. A. Pandit, S. A. Bhat and M. A. Bhat, *Talanta*, 2015, 131, 55-58.
- 3 E. Josef and H. Bianco-Peled, *Soft Matter*, 2012, 8, 9156-9165.
- 4 E. Buhler and F. Boué, *Macromolecules*, 2004, 37, 1600-1610.
- 5 J. Combet, P. Lorchat and M. Rawiso, *Eur. Phys. J.: Spec. Top.*, 2012, 213, 243-265.
- 6 P. Sharp and V. A. Bloomfield, *Biopolymers*, 1968, 6, 1201-1211.
- 7 J. des Cloizeaux, *Macromolecules*, 1973, 6, 403-407.

- 8 M. Shimode, M. Mimura, H. Urakawa, S. Yamanaka and K. Kajiwara, *Sen'i Gakkaishi*, 1996, 52, 301-309.
- 9 I. Dogsa, J. Štrancar, P. Laggner and D. Stopar, *Polymer*, 2008, 49, 1398-1406.
- 10 J. Teixeira, *J. Appl. Crystallogr.*, 1988, 21, 781-785.
- 11 B. Hammouda, *J. Appl. Crystallogr.*, 2010, 43, 716-719.